RESEARCHERID
THOMSON REUTERS

[Okegbola* 7(6): June, 2020] ISSN 2349-4506
Impact Factor: 3.799

Global Journal of Engineering Science and Research Management

GEOMETRIC ACCURACY ASSESSMENT OF UAS-BASED ORTHOPHOTOS AND GNSS OBSERVATIONS USING RTK MODE

Michael Oketunde OKEGBOLA*, Somtoochukwu Chukwunonso OKAFOR, Segun Muyiwa OLUDIJI, Ganiyu O. RAHEEM, Mutairu Abdulwaheed YUSUF

* Department of Surveying and Geoinformatics, Federal School of Surveying, Oyo, Oyo State, Nigeria
Department of Surveying and Geoinformatics, Federal School of Surveying, Oyo,
Oyo State, Nigeria
Department of Geoinformatics and Surveying, University of Nigeria, Enugu Campus, Enugu State, Nigeria.
Department of Surveying and Geoinformatics, The Oke-Ogun Polytechnics, Shaki, Oyo State, Nigeria.
Department of Surveying and Geoinformatics, Federal Polytechnic, Nekede, Imo State, Nigeria.

DOI: 10.5281/zenodo.3895574

KEYWORDS: UAS, GNSS, Geometric Accuracy, Image, Map generation, Geometric Quality

ABSTRACT

This paper attempts to research and investigate geometric quality of an Unmanned Aerial Orthophoto from DJI Phantom 4 Pro for map generation and compilation despite the fact that a fewer number of control points were used and this was then compared with same points as observed from a Hi Target V30 GNSS Receiver in Real Time Kinematic (RTK) mode. Two important criteria are pivotal to Geometric quality assessment of an Aerial photograph; Geometric accuracy and Object-definition property while this research focused on the geometric accuracy as compared to another method of terrestrial data acquisition using GNSS. In remote sensing and photogrammetric operations, the geometric quality of the imagery purely depends on the relation between pixel size and the map scale including contrast information, atmospheric condition, the sun elevation, the printing technology and the screen resolution. The Unmanned Aircraft System (UAS) deliverables which include the Orthophoto and the Digital Surface Model (DSM) among other deliverables like Digital Elevation Model, Point Cloud etc. shows that UAS (Phantom 4 Pro) can be used for compilation of large scale maps in partly accessible or inaccessible areas according to the map accuracy analysis of the National Standard for Spatial Data Accuracy (NSSDA). The horizontal accuracy of 3.207m (RMSE: 1.85m) and vertical accuracy of 0.884m (RMSE: 0.45m) were obtained and also compared with the corresponding results from the RTK observations in DGNSS and falls within the allowable misclosure, hence, suitable for Cadastral mapping procedures and compilation.

INTRODUCTION

Mapping is a tedious job especially when it comes to large area of coverage. Methods of ground surveying, photogrammetry, cartography and other terrestrial methods employed in the years past for data capture, processing, presentation and storage are rigorous, time consuming and limited in capacity. Global Navigation Satellite System (GNSS) is one of the methods used for position determination and navigation using satellites and GNSS Receivers which ranges in system developments from different countries like US (GPS), Russia (GLONASS), EU and ESA (Galileo), China (COMPASS) etc. Recently, there have been increasing interests in the UAVs applications such as surveillance, search and rescue, object detection and mapping [10]; [11].

In analog photogrammetry, orthophotos, topographic maps and other map deliverables have been produced from the aerial photographs acquired using the large format metric cameras. The cost of acquiring these cameras and aerial photographs through the traditional means such as manned aircrafts is relatively high and requires critical planning. Although, large format aerial cameras are very useful for mapping large area but the advancement in technology has made the use of small format digital cameras advantageous in achieving same purpose [1]. The small format digital camera has shown great relevance and applications in researches throughout the world for mapping purposes such as topographical mapping and other applications such as land slide mapping, map revision, image spectral mapping, research and civil engineering designs etc. [1]. These small format digital camera offer several advantages above large format metric camera and some of these advantages include the portability,

accessibility, ease of use and reduction in cost above all to mention but a few [9], although analysis of the cost for data acquisition methods using the small format camera is not capture in this research.

So, in this study, a Quadcopter Unmanned Aerial System (Phantom 4 Pro) equipped with a calibrated small format and fixed digital camera, Global Positioning System (GPS), tracking system and Inertial Navigation System (INS) forms the data acquisition system of the platform/payload. A Quadcopter UAV, also known as a quadrotor, is one type of UAV, which is lifted and propelled by four rotors/propellers. The quadcopter has high maneuverability, as it can hover, take off, cruise and land in narrow areas. Quadcopters have simpler control mechanism both in manual and autonomous flight modes compared to the other fixed wing UAVs [10]; [4]. Establishment of Ground Control Points (GCPs) using Hi-Target V30 GNSS receivers helped in improving the geometric quality/georeferencing during the processing of the data to obtain a referenced Orthophoto, Point Cloud and a Digital Surface Model (DSM) which was done using Agisoft Metashape from DJI Company. This paper hence research the suitability of the data acquired by (UAV) which is aerial method (digital photogrammetry and remote sensing) compared to data acquired using GNSS in RTK mode which in the other hand is a terrestrial method through the presentation of geometric quality analysis of the deliverables from both methods.

1.1 Unmanned Aircraft System (UAS)

An unmanned aerial vehicle (UAV) like receivers in GPS is just a component of a system called Unmanned Aircraft System (UAS); which include a UAV, a ground-based controller, and a system of communications between the two. UAV/DRONE is therefore a high-tech Dynamic Remotely Operated Navigation Equipment (DRONE) or aircraft without a human pilot aboard. The flight of UAVs may operate with various degrees of autonomy: either under remote control by a human operator or autonomously by onboard computers [12]. The term Unmanned Aerial/Aircraft System (UAS) is frequently used in the Engineering, Computer Science, Robotics and Artificial Intelligence, Photogrammetry and Remote Sensing world. Besides names like Remotely Piloted Vehicle (RPV) which was first used in 1970, Remotely Operated Aircraft (ROA) or Remotely Piloted Aircraft (RPA) are used by various authors and researchers [4]. Several terms such as ROA and RPA have been used by National Aeronautics and Space Administration (NASA) and Federal Aviation Administration (FAA) in the U.S. in place of Unmanned Aerial Vehicle (UAV) which was first used in 1986 [3].

The Unmanned Vehicle Systems International Association has explicitly defined the remotely controlled and model helicopters as mini, close and medium range UAVs depending on their flight strength, size and flying height range [5]. UAS, as used in photogrammetry and remote sensing stands for the whole system, including the Unmanned Aircraft or Unmanned Vehicle (UA/UV) with the Sensor on-board, radio link/communication and the Ground Control Station or Ground Controller (GCS/GC). UAVs, in contrast to Manned Aircraft Systems (MAS) have some major advantages. UAVs can be used in high risk situations without endangering human lives and inaccessible areas, at low altitude and at flight profiles close to the objects where manned systems cannot hover (Eisenbeiss, 2004). These locations include natural and artificial disaster sites like mountainous and volcanic areas, mud slides, oil spillage, flood plains, earthquake and desert areas and scenes of accidents [2]. The implementation of Global Positioning System and or Inertia Navigation System (GPS/INS) incorporated in the built of UAS/UAV systems has helped in the stabilization and navigation of the units to allow precise flights, ensuring on the one hand sufficient and adequate image coverage and overlap, enabling the robustness of flight planning process, especially the INS through the Inertial Measuring Unit (IMU) to guide the UAVs navigation movement in the cases of minimum satellite loss during operation for navigation and positioning. The INS accelerometers in xyz (yaw, pitch and roll) filled the gap.

Based on latest development by DJI Company, a Phantom 4 UAV has been invented among others (See Fig. 1). This system is capable of generating three main survey deliverables namely Orthomosaic, digital terrain/surface model (raster elevation) and point cloud maps.

ISSN 2349-4506
Impact Factor: 3.799
Global Journal of Engineering Science and Research Management

Fig. 1. DJI Phantom 4 Pro (Complete UAS)

STUDY AREA

The study area lies within Part of Ladigbolu Layout in Oyo West Local Government Area, Oyo, Oyo State, Nigeria. It falls approximately between the geographic coordinates of Latitudes 07° 49' 11".02 N, 07° 49' 29".40 N and Longitudes 03° 54' 41".13 E, 03° 55' 13".53 E.

Fig. 2. Location of the study area, part of Ladigbolu Layout

RESEARCH METHODOLOGY

3.1 Establishment of Ground Control Points

Seven (7) Ground Control Points (GCPs) including two check (CHKPTs) points were established using Hi-Target V30 in static mode of observation and these were used for georeferencing and check of the processing. See Fig. 6 for a sample Ground Control Point (GCP) established and marked before flight.

Table 1: Established Ground Control Points (GCPs) and Check Points (CHKPTs) with Hi Target V30

ID	Easting (Meter)	Northing (Meter)	Elevation (Meter)	Feature Code
GCP1	601335.979	864537.056	307.599	Rover
CHKPT2	601101.836	864553.816	300.593	Rover
GCP3	600901.781	864596.037	294.237	Rover
GCP4	600655.329	864741.219	284.576	Rover

CHKPT5	600799.268	864826.965	288.331	Rover
GCP6	601087.574	864730.156	296.359	Rover
GCP7	601205.823	864707.031	298.644	Rover
XSN_07	604755.785	866879.146	309.972	BASE

3.2 Initial Flight Planning

The initial flight planning of the study area was carried out in DroneDeploy software (Fig. 4 and 5) but the type/model of drone was initially selected in DJI GO 4 (Fig. 3). DroneDeploy software has the google map and imagery tiles embedded which shows the locations by search or navigation once online and the name of the location of interest is supplied or manually navigated to. This was used to define the flight boundary which otherwise brings a default flight lines including the front and side overlap values which was later changed to desired values and this planning was sent and uploaded to the drone. Altitude of 100m was selected for the flying height having considered dangerous obstructions such as cell towers, power lines or other objects that could impede the flight plan, front/side overlap was 75/65% respectively and the drone flew according to the plan. It took approximately 25 minutes to cover the study area of about 40 Hectares with a total number of 457 images planned on eleven (11) main flight lines on an average speed of 10m/s using two (2) batteries, the ground resolution was 3.43cm/pixel on a pixel size of 2.61 x 2.61µm.

A suitable leveled ground within the study area was selected for save vertical takeoff and landing of the autonomous flight and having considered all the necessary precautions and flight controls, the UAV was flown as earlier planned with the fact that there was no flight restriction over the study area.

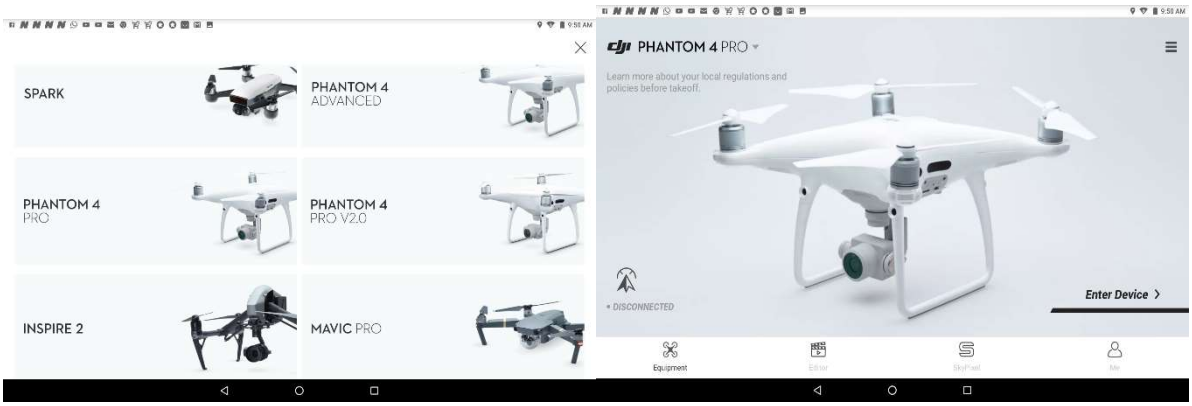

Fig. 3: Selecting Type of drone used in DJI Go 4 Software (Phantom 4 Pro)

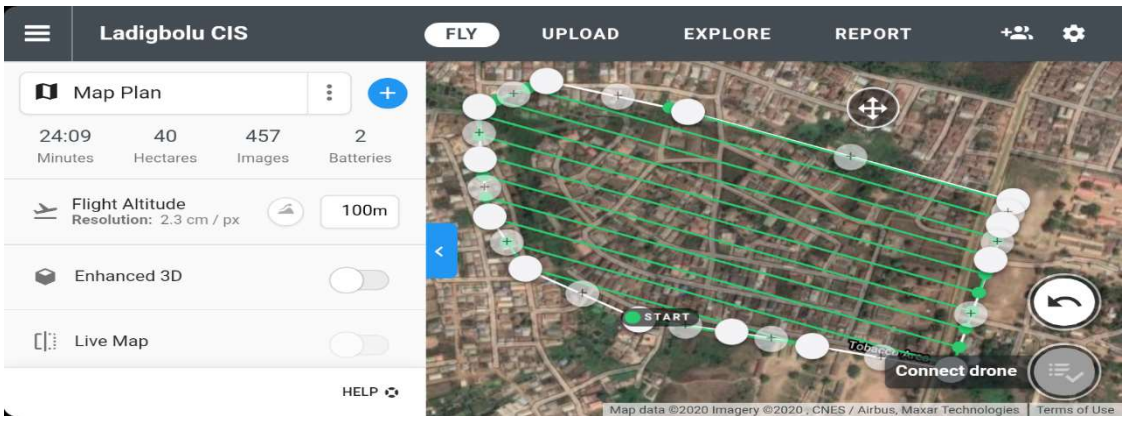

Fig. 4: Flight Planning in Drone Deploy Software showing Settings for Flight Altitude

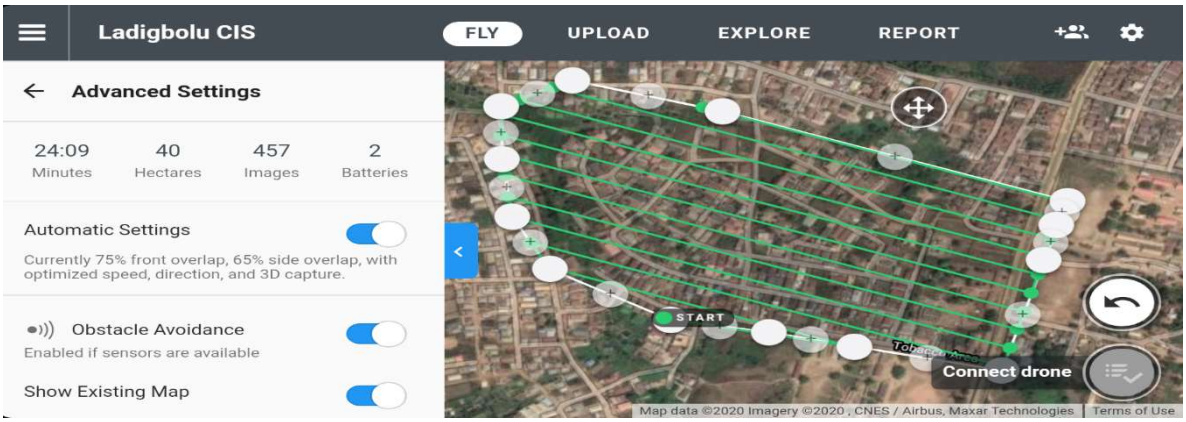

Fig. 5: Flight Planning in Drone Deploy Software showing Settings for overlaps

Fig. 6: A sample GCP (As placed on a concrete 18 X 18cm concrete beacon)

3.3 Data Collection/Image Acquisition with UAV

A single flight plan was used to cover the study area with two (2) batteries and the wind direction was automatically considered at an angle of 40 degrees. Take-off and landing position was defined approximately at the centre of the study area in a relative clear and levelled surface. In preparation of the flight the Ground Remote Controller (GRC) was switched on and later the UAV, when the communication has been established, then the DJI GO 4 was launched to select the type of drone to be used i.e Phantom 4 Pro and then the software displayed "CONNECTED" once the drone was detected, the software was then minimized and DRONEDEPLOY software was launched then once the drone is detected and the connection is established "Drone Connected" is displayed" and Ladigbolu CIS Project which has been earlier planned (Fig. 3&4) was opened and "Start preflight checklist" was clicked and while the software carry out some preflight checks, the flight plan was automatically uploaded into the drone then "Start flight" was clicked for the "Autonomous flight", the drone then take off and register the take off point by taking a camera position of the point then fly to the specified flight height and then horizontally fly to the starting point before it finally fly through the predefined flight lines to capture all the images/camera positions considering the pre-configuration parameters like the overlaps, speed etc. Finally, after all the lines had been flown the drone returns and lands approximately on same take-off point and it was switched off.

3.4 Image/Data Processing

Agisoft Metashape was used for the processing of the captured images using the drone after all had been downloaded and added in Agisoft Metashape from DJI for further processing, above all for a mosaic building to generate the Orthophoto (see Table 2) for image properties as extracted from the processing reports. The processing is the most time-consuming as compared to acquisition which is fun filled, the procedure ranges from importing of image files, photo alignment, importing of tie point files for georeferencing and adjustments, Placement of Markers for referencing, building of dense cloud, Building of Mesh, Texture and tiled model,

Building of Digital Elevation Model (DSM/DEM as the case may be) and finally, the building of Orthophoto. The software was running on an HP workstation with the following configuration properties; 16GB RAM, Intel® Core™ i7 @ 3.50GHz processor, 64Bits operating system and 1TB hard drive disk. The data was post-processed in UTM 31N projected coordinate system referenced to the WGS84 global ellipsoid. Five (5) GCPs were used for the adjustment of Tie points (Aero-triangulation) succeeded by the production of Digital Elevation Model and Orthophoto while two (2) CHKPTs were used to check the processing accuracy compared to the values of the points observed with GNSS receivers and that of same points extracted from the UAV Orthophoto.

Table 2: Image Data Properties

Item	**Description**
Image dimension (Pixel)	4864 x 3648
Pixel Size (µm)	2.61 x 2.61
Ground Resolution (per pixel)	3.43cm
Image Format	Tiff
Ground Dimension of the image	90,056 x 52,656
Number of images Acquired	457

RESULTS AND ANALYSIS

These contains the various deliverables obtained in the course of the data acquisition and data processing. It involves the measurement of the Geometric accuracy of the Orthomosaic after the performance of aerial triangulation (adjustment of tie points) and map generation respectively.

4.1 Results: The raster elevation map was used to generate Digital Surface Models such as contour map in ArcGIS as well as 3D wireframe in Surfer 10, reports of the processing as well as the coordinate summary including that of the Orthophoto and the DEM were all generated by Agisoft Metashape.

Fig. 7. Orthophoto generated in Agisoft Metashape

4.2. Analysis: The positional accuracy of the Orthomosaic map was considered using the check points, the linear accuracy by linear measurements on the map related and compared to ground measurement as measured with GNSS receiver in RTK mode, the spatial resolution of the Orthophoto map obtained was also analyzed as seen in the subsequent subsection.

4.2.1. Quantitative Analysis: Quantitative analysis deals with assessment of the values obtained using suitable statistical tools right from the report generated in Agisoft Metashape. This aspect of the analysis was actualized by computing the root mean square error.

$$RMSE = \sqrt{\frac{\Sigma(N_i - N_j)^2}{n}}$$

(Source, [6]).

Where, Ni = Observed values, Nj = Reference values and n = Number of points or stations The check points used for this project were the control points within the flight area established for other purposes. Table 4 shows the check points having the map horizontal accuracy 0.451459mm and vertical accuracy of 0.0513604mm with a total RMSE of 0.309mm. Aligned with the National Standard for Spatial Data Accuracy [6] in Geospatial Positioning Accuracy Standards.

Table 3. Summary of Control Points Root Mean Square Error (RMSE)

Label	XY error (mm)	Z error (mm)	Projections	Error (pix)
GCP 1	0.0485443	0.00324679	9	0.265
GCP 3	0.106137	-0.00225861	13	0.336
GCP 4	0.0600336	0.00263777	14	0.263
GCP 6	0.0532834	0.00472018	12	0.294
GCP 7	0.0486907	-0.00564057	12	0.357
Total	**0.066986**	**0.00391655**		**0.306**

X – Easting, Y – Northing, Z – Altitude
Source: Author's field work report, Year 2020

Table 4. Summary of check points Root Mean Square Error (RMSE)

Label	XY error (mm)	Z error (mm)	Projections	Error (pix)
CHKPT 2	0.598488	0.0585917	10	0.354
CHKPT 5	0.222358	0.0429279	14	0.273
Total	**0.451459**	**0.0513604**		**0.309**

X – Easting, Y – Northing, Z – Altitude
Source: Author's field work report, Year 2020

Table 5. GNSS observed values on sampled points (Including all GCPs and Checkpoints)

Version : 1											
Name	N	E	Z	B	L	H	Antenna H	Nrms	Erms	Zrms	Solution Type
GCP1	864537.060	601335.989	307.601	7:49:12.909	3:55:08.885	319.421	1.877	0.008	0.011	0.033	RTKInt
ckpt2	864553.813	601101.839	300.600	7:49:13.467	3:55:01.241	315.411	1.877	0.007	0.006	0.012	RTKInt
GCP3	864596.027	600901.781	294.249	7:49:14.856	3:54:54.713	308.716	1.877	0.007	0.006	0.012	RTKInt
GCP4	864741.217	600655.309	284.590	7:49:19.601	3:54:46.676	298.646	1.877	0.007	0.006	0.013	RTKInt
ckpt5	864826.955	600799.248	288.320	7:49:22.382	3:54:51.381	303.750	1.877	0.007	0.006	0.013	RTKInt
GCP6	864730.154	601087.595	296.371	7:49:19.210	3:55:00.789	311.790	1.877	0.007	0.006	0.013	RTKInt
GCP7	864707.011	601205.835	298.689	7:49:18.448	3:55:04.648	309.005	1.877	0.007	0.006	0.013	RTKInt
RTK8	864879.999	601054.242	287.997	7:49:24.091	3:54:59.711	301.324	1.877	0.007	0.006	0.013	RTKInt
RTK9	864563.756	601621.203	300.221	7:49:13.754	3:55:18.199	314.257	1.877	0.007	0.006	0.013	RTKInt
RTK10	864798.443	601165.444	300.229	7:49:21.428	3:55:03.336	315.192	1.877	0.007	0.006	0.013	RTKInt

N – Northing, E – Easting, Z – Ortho. Height, B – Latitude, L – Longitude, H – Ellip. Height
Source: Author's field work report, Year 2020

4.2.2. Qualitative Analysis

Qualitative assessment of the Orthophoto was done by comparing the results obtained from the two methods, see Table 6. And finally the coordinates of the Established GCP was compared with that which was extracted from the Orthophoto. (XY from the Orthophoto and Z from the DEM) using ArcGIS 10.1, then the root mean square errors was computed using excel program for difference in x, y and z to obtain the final RMSE in horizontal and vertical. see the result as shown in Table 7.

Table 6. Comparing coordinates of sampled Points using GNSS RTK and Orthomosaic (same points)

CHECK POINT IDs		ORTHOPHOTO RESULT			GNSS RESULT IN RTK MODE			DIFFERENCE		
ID RTK	ID Orthophoto	N	E	H	N	E	H	ΔN	ΔE	ΔH
GCP1	PH 01	864537.060	601335.989	307.601	864537.089	601335.978	307.499	-0.029	0.011	0.102
ckpt2	PH 02	864553.813	601101.839	300.600	864553.835	601101.872	300.653	-0.022	-0.033	-0.053
GCP3	PH 03	864596.027	600901.781	294.249	864595.995	600901.815	294.298	0.032	-0.034	-0.049
GCP4	PH 04	864741.217	600655.309	284.590	864741.205	600655.299	284.558	0.012	0.01	0.032
ckpt5	PH 05	864826.955	600799.248	288.320	864826.988	600799.239	288.317	-0.033	0.009	0.003
GCP6	PH 06	864730.154	601087.595	296.371	864730.133	601087.563	296.376	0.021	0.032	-0.005
GCP7	PH 07	864707.011	601205.835	298.689	864707.000	601205.865	298.595	0.011	-0.03	0.094
RTK8	PH 08	864879.999	601054.242	287.997	864879.973	601054.231	287.965	0.026	0.011	0.032
RTK9	PH 09	864563.756	601621.203	300.221	864563.797	601621.182	300.432	-0.041	0.021	-0.211
RTK10	PH 10	864798.443	601165.444	300.229	864798.411	601165.475	300.552	0.032	-0.031	-0.323
								0.0007525	0.0005994	0.017538
					ROOT MEAN SQUARE ERROR					
			HORIZONTAL =		0.0013519	X	0.004515	=	6.103E-06	
			VERTICAL =		0.0175382	X	0.005136	=	9.008E-05	

Source: Author's field work report, Year 2020

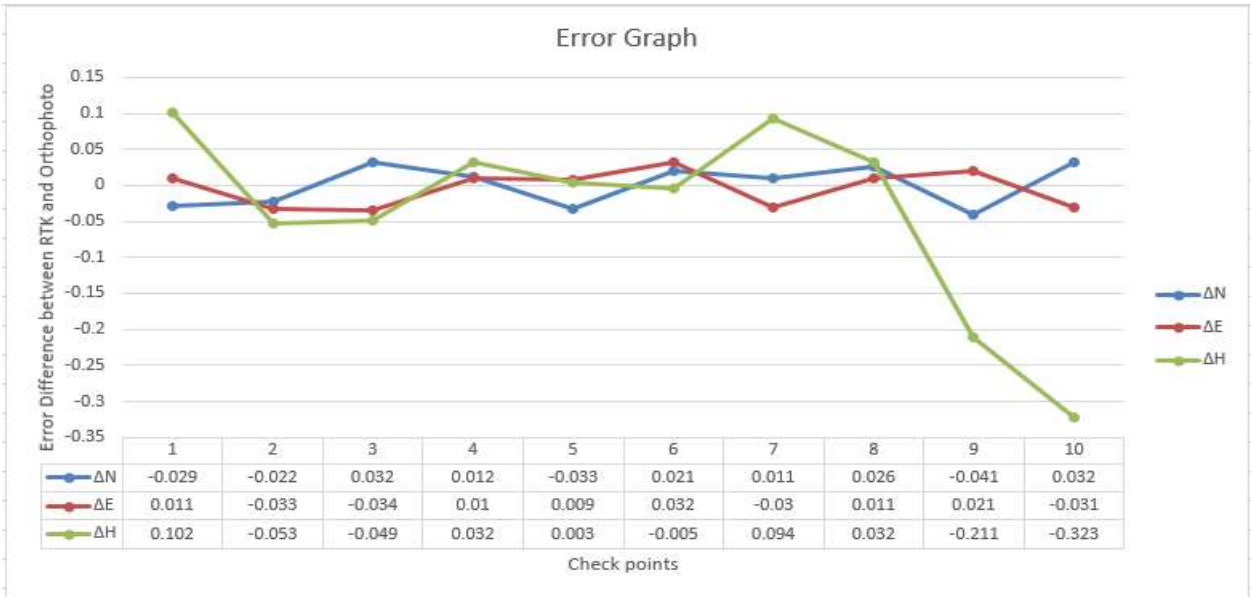

	1	2	3	4	5	6	7	8	9	10
ΔN	-0.029	-0.022	0.032	0.012	-0.033	0.021	0.011	0.026	-0.041	0.032
ΔE	0.011	-0.033	-0.034	0.01	0.009	0.032	-0.03	0.011	0.021	-0.031
ΔH	0.102	-0.053	-0.049	0.032	0.003	-0.005	0.094	0.032	-0.211	-0.323

Fig. 8 Graph plot of the difference between RTK and Orthophoto coordinates

Using the following formulas Table 6 and 7 was obtained.

$$RMSE_X = \sqrt{\sum (X_i - X_j)^2/n}$$

To get the RMSE in Easting

$$RMSE_Y = \sqrt{\sum (Y_i - Y_j)^2/n}$$

To get the RMSE in Northing

$$RMSE_r = \sqrt{\sum[(X_i - X_j)^2 + (Y_i - Y_j)^2]/n} = \sqrt{(RMSE_X)^2 + (RMSE_Y)^2}$$

To get the RMSE in Horizontal

$$RMSE_Z = \sqrt{\sum (Z_i - Z_j)^2/n}$$

To get the RMSE in Vertical

Table 7. Computation of the RMSE in Horizontal and Vertical

CHECK POINT IDs		GNSS RESULT IN RTK MODE			ORTHOPHOTO RESULT			DIFFERENCE		
ID RTK	ID Orthophoto	N	E	H	N	E	H	ΔN	ΔE	ΔH
GCP1	PH 01	864537.060	601335.989	307.601	864537.089	601335.978	307.499	-0.029	0.011	0.102
ckpt2	PH 02	864553.813	601101.839	300.600	864553.835	601101.872	300.653	-0.022	-0.033	-0.053
GCP3	PH 03	864596.027	600901.781	294.249	864595.995	600901.815	294.298	0.032	-0.034	-0.049
GCP4	PH 04	864741.217	600655.309	284.590	864741.205	600655.299	284.558	0.012	0.01	0.032
ckpt5	PH 05	864826.955	600799.248	288.320	864826.988	600799.239	288.317	-0.033	0.009	0.003
GCP6	PH 06	864730.154	601087.595	296.371	864730.133	601087.563	296.376	0.021	0.032	-0.005
GCP7	PH 07	864707.011	601205.835	298.689	864707.000	601205.865	298.595	0.011	-0.03	0.094
RTK8	PH 08	864879.999	601054.242	287.997	864879.973	601054.231	287.965	0.026	0.011	0.032
RTK9	PH 09	864563.756	601621.203	300.221	864563.797	601621.182	300.432	-0.041	0.021	-0.211
RTK10	PH 10	864798.443	601165.444	300.229	864798.411	601165.475	300.552	0.032	-0.031	-0.323
								0.0007525	0.0005994	0.017538
					ROOT MEAN SQUARE ERROR					
			HORIZONTAL =		0.0013519	X	0.004515	=	6.103E-06	
			VERTICAL =		0.0175382	X	0.005136	=	9.008E-05	

Source: Author's field work report, Year 2020

Table 8. Comparison of GCP as established with GNSS in Static with Orthophoto extraction

CHECK POINT IDs		GNSS RESULT IN STATIC MODE			ORTHOPHOTO RESULT			DIFFERENCE		
ID STATIC	ID Orthophoto	N	E	H	N	E	H	ΔN	ΔE	ΔH
GCP1	PH 01	864537.056	601335.979	307.599	864537.060	601335.989	307.601	-0.004	-0.010	-0.002
CHKPT2	PH 02	864553.816	601101.836	300.593	864553.813	601101.839	300.600	0.003	-0.003	-0.007
GCP3	PH 03	864596.037	600901.781	294.237	864596.027	600901.781	294.249	0.010	0.000	-0.012
GCP4	PH 04	864741.219	600655.329	284.576	864741.217	600655.309	284.590	0.002	0.020	-0.014
CHKPT5	PH 05	864826.965	600799.268	288.331	864826.955	600799.248	288.320	0.010	0.020	0.011
GCP6	PH 06	864730.156	601087.574	296.359	864730.154	601087.595	296.371	0.002	-0.021	-0.012
GCP7	PH 07	864707.031	601205.823	298.644	864707.011	601205.835	298.689	0.020	-0.012	-0.045

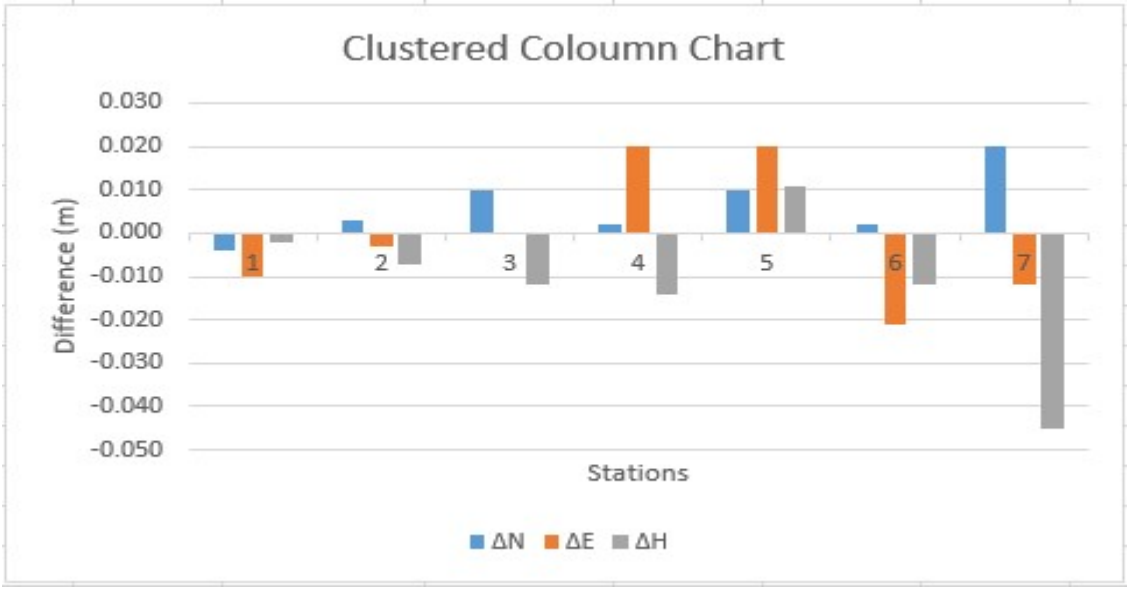

Fig. 9 Graph plot of the difference between Static GCP and Orthophoto GCP coordinates

CONCLUSION

While preference is being encouraged and given to technological advancement in the area of digital photogrammetry and remote sensing, the realms of software and hardware intelligence makes them competitive. So, it will be good to highlight and appraise the solution providers in these areas and also spice up the developers by exhibiting what their products are capable of even when they have not really emphasized them at the time of production and this will help them to further improve on the components of their respective software and hardware where necessary. In this study, Orthophoto, DEM and point cloud were successfully generated from photogrammetric data using Agisoft Metashape. Thus, conclusions can be made from the results and analysis obtained that the Unmanned Aircraft System Orthophoto is accurate enough and can be likened to the accuracy obtained using GNSS RTK receivers. While the Orthophotos can be employed in property surveys ranging from as-built, detail, for updating and revision of topographic maps with minimal number of GCPs and a high percentage of forward and side overlaps (Gruber, et al., 2004). While we cannot over emphasize the suitability of UAVs in inaccessible areas the map accuracies in horizontal and vertical RMSE and differences as shown in tables and figures are enough to conclude here that Orthophoto generated from Agisoft Metashape should be employed in order to achieve accurate mapping because it falls below the maximum allowable RMSE according to the American Society for Photogrammetry and Remote Sensing [8]; [6]. The geometric quality through geometric accuracy in Table 7 and the resolution/metadata of the Orthophoto makes it fit for topographical map compilation, engineering survey maps and cadastral maps, agriculture and forestry in areas such as crop population/growth monitoring, forest classification and vegetation health mapping respectively, even in Image spectral mapping using RGB bands only for shoreline mapping [12].

ACKNOWLEDGMENTS

The authors appreciate the Rector, HOD including SIWES and Practical's Coordinator Surveying and Geoinformatics department, Federal School of Surveying, Oyo for assisting this research with the school's UAS.

REFERENCES

1. Ahmad, A. (2006), Digital photogrammetry: An experience of processing aerial photograph of UTM acquired using digital camera, accessed online at https://www.researchgate.net/publication/228739845_Digital_Photogrammetry_An_Experience_Of_Processing_Aerial_Photograph_Of_UTM_Acquired_Using_Digital_CAMERA on 23/10/2019)

2. Ahmad, A. (2011), Digital Mapping Using Low Altitude UAV, Pertanika J. Sci. & Technol., accessed online at https://www.researchgate.net/publication/266868746_Digital_mapping_using_low_altitude_UAV on 23/01/2020.
3. Colomina, I., Blázquez, M., Molina, P., Pares, M. E. and Wis (2008), Towards A New Paradigm for High-Resolution Low-Cost Photogrammetry and Remote Sensing, *The International Archives of the Photogrammetry, Remote Sensing and Spatial Information Sciences, ISPRS Congress. Beijing, China, XXXVII. Part B1*, pp. 1201-1206.
4. Daramola, O., Olaleye, J., Ajayi, O. G. and Olawuni, O. (2017), Assessing the geometric accuracy of UAV-based Orthophoto, *South African Journal of Geomatics*, DOI: http://dx.doi.org/10.4314/sajg.v6i3.9, Vol. 6. No. 3, pp. 395-396.
5. Eisenbeiss, H. (2004), A Mini Unmanned Aerial Vehicle (UAV): System Overview and Image Acquisition, International Workshop on Processing and Visualization Using High-Resolution Imagery. Pitsanulok, Thailand, 2004 (accessed online at https://www.researchgate.net/publication/228788846_A_mini_unmanned_aerial_vehicle_UAV_system_overview_and_image_acquisition on 29/01/2020).
6. FGDC, NSSDA. (1998). "Geospatial Positioning Accuracy Standards." Virginia: Federal Geographic Data Committee, (accessed online at https://www.fgdc.gov/standards/projects/FGDC-standards-projects/accuracy/part3/chapter3, on 15th January, 2020).
7. Gruber, M., Roland P., and Martin P. (2004), The all Digital Photogrammetric workflow: Redundancy and Robustness, *ISPRS Commission I: Sensors, Platforms and Imagery*, pp. 232-234.
8. Lawali, R., and Waziri A. D. (2014), Digital Orthophoto Generation with Aerial Photographs, *Academic Journal of Interdisciplinary Studies, MCSER Publishing* 3, pp. 2281-3993.
9. Mikrut, S. (2016), Classical Photogrammetry and UAV-Selected Aspects, The International Archives of the photogrammetry, Remote sensing and Spatial Information Sciences, XLI-B1.
10. Mohammed, R., Ali R., Muhammad, T., Kang-Hyun N. and Sung, H. K. (2018). Autonomous Vision-based Target Detection and Safe Landing for UAV, *International Journal of Control, Automation and Systems*, ISSN:1598-6446, 16(6), pp. 3013-3014.
11. Okegbola, M. O., Ajisafe, B. I., Olaosegba, S. O. and Okegbola, S. A. (2019). UAV Image Mapping: An Application in Monitoring and Control of Crime and Insecurity, *Global Journal of Engineering Science and Research Management*, DOI: 10.5281/zenodo.3559660, ISSN 2349-4506, 6(11), pp. 20-21.
12. Okegbola, M. O. and Okegbola, S. A. (2020). "Unmanned Aerial System Application in Spectral Image Mapping of Part of Erelu Dam Shoreline and Vegetation Index Pattern in Oyo, Oyo State", *Conference list of Abstract and proceedings of Annual General Meeting/Conference of the National Association of Surveying and Geoinformatics Lecturers (OYO 2020)*, (accessed online at https://www.researchgate.net/publication/341520675_UASUAV_APPLICATION_IN_SPECTRAL_IMAGE_MAPPING_OF_PART_OF_ERELU_DAM_SHORELINE_AND_VEGETATION_INDEX_PATTERN_IN_OYO on 23/01/2020).